OPEN ACCESS
JOURNAL OF ADVANCED DIELECTRICS
Vol. 13, No. 5 (2023) 2350014 (9 pages)

DOI: 10.1142/S2010135X23500145

High entropy dielectrics

Liangchen Fan, Yuanxun Li, Jie Li, Quanjun Xiang, Xiaohui Wang,
Tianlong Wen, Zhiyong Zhong and Yulong Liao*
State Key Laboratory of Electronic Thin Films and Integrated Devices
University of Electronic Science and Technology of China
Chengdu 611731, P. R. China
*yulong.liao@uestc.edu.cn

Received 11 February 2023; Revised 28 March 2023; Accepted 24 April 2023; Published 5 July 2023

High entropy oxides (HEO) are single-phase solid solutions which are formed by the incorporation of five or more elements into a cationic sublattice in equal or near-equal atomic proportions. Its unique structural features and the possibility of targeted access to certain functions have attracted great interest from researchers. In this review, we summarize the recent advances in the electronic field of high-entropy oxides. We emphasize the following three fundamental aspects of high-entropy oxides: (1) The conductivity mechanism of metal oxides; (2) the factors affecting the formation of single-phase oxides; and (3) the electrical properties and applications of high-entropy oxides. The purpose of this review is to provide new directions for designing and tailoring the functional properties of relevant electronic materials via a comprehensive overview of the literature on the field of high-entropy oxide electrical properties.

Keywords: High entropy dielectrics; conductive mechanisms; electrical properties; dielectric constant.

1. Introduction

Entropy is a thermodynamic parameter that indicates the degree of disorder or chaos in a material. Entropy is influenced by temperature, the number of elements and the atomic fraction of each element in the composition. The relationship between the atomic fraction of an element and the entropy of a mixture is shown by the following equation.[1]

$$\Delta S_{mix} = -R\sum_{i=1}^{N} X_i \ln X_i, \quad (1)$$

where R, N and X_i are the ideal gas constant, the number of components and the atomic fraction of component i, respectively.

In 2004, Yeh *et al*.[2] first introduced the concept of high entropy alloys (HEAs) based on the principle that the constitutive entropy of mixing (ΔS_{mix} in Eq. (1)) increases with the addition of more equimolar elements to the alloy system. Recently, a series of new ceramic materials derived from high-entropy alloys, so-called high-entropy oxides (HEOs), have attracted intensive scholarly research interest. The growing interest in the field of HEOs is reflected in the large number of studies focusing on their different structural and functional aspects, which have been reported within five years of their discovery.[3–6] In highly disordered multicomponent systems, HEOs trigger a series of very attractive features, including the tendency to form solid solutions with a single-crystal structure, properties beyond their constituents and the possibility to modulate their functional properties.[7–11] HEOs have different crystal structures, including rock salt,[12,13] fluorite,[14] chalcocite,[15,16] pyrochlore,[17] spinel,[18–20] etc. In addition, they have remarkable properties for applications in thermal and environmental protection,[21,22] thermoelectricity,[23] hydrolysis,[24] catalysis[25–27] and energy storage.[28–31] For example, Zhao *et al*. prepared a high-entropy $(Ca_{0.2}Sr_{0.2}Ba_{0.2}La_{0.2}Pd_{0.2})TiO_3$ perovskite. The presence of numerous boundaries and the ultra-dense discontinuous lattice produce significant interfacial and dipole polarization. Meanwhile, the superdense strain originating from the severe lattice distortion of this high entropy composition provides a strong transport capacity for the electron carriers and promotes dielectric dissipation. Thus, the EAB increases from 0.7 GHz to 1.4 GHz and the bandwidth of $(Ca_{0.2}Sr_{0.2}Ba_{0.2}La_{0.2}Pd_{0.2})TiO_3$ is increased by nearly two times over $BaTiO_3$.[32] Kheradmandfard *et al*. fabricated entropy-stabilized $(Mg_{1/5}Cu_{1/5}Ni_{1/5}Co_{1/5}Zn_{1/5})$ O-oxides by a new ultra-fast green microwave-assisted technique, and the work demonstrates that this material shows excellent lithium storage performance (i.e., reversible capacity can exceed 250 mA/g at 5 A/g).[33] Wang *et al*. recently prepared a high-entropy oxide $(Co, Cr, Fe, Mn, Ni)_3O_4$ with spinel structure for Li-ion batteries and obtained high capacity (discharge/charge, 1034/680 mAh g^{-1}) and excellent cycling performance, which was attributed to the stabilizing effect of entropy during the intercalation/de-lamination of Li^+.[34]

*Corresponding author.

Many aspects of high entropy oxides (HEO), such as high entropy-based nomenclature, synthesis methods, associated thermodynamic parameters, phase structures and some functional characteristics, have been highlighted in several review articles. The focus of this paper is on the electrical properties of HEO. The conductivity mechanisms of metal oxides associated with high-entropy oxide materials are briefly discussed. The factors that influence the synthesis of single-phase oxides are summarized. A summary of the electrical properties in less researched high-entropy oxide materials is provided. At last, we present our views on the future direction of electrical properties research to provide new directions for the design of electronic materials with excellent performance.

2. Conductive Mechanisms in Metal Oxides

For traditional gallium (GaAs), indium phosphide (InP), etc., their conductive behavior can be perfectly described by the energy band theory based on the single-electron approximation, i.e., their conductivity is generated by the directional migration of carriers (electrons or holes) in the conduction and valence bands.[35,36] However, there have been great obstacles in using energy band theory to explain the conductive properties of transition metal oxides. For example, when explaining the conductivity of nickel oxide (NiO), according to the energy band model, ionic crystals of sodium chloride structure should be conductors owing to their unfilled valence band, but the resistivity measured at room temperature is as high as 5×10^{14} Ω·cm. Similarly, MnO should be a conductor owing to its unfilled valence band, but it is experimentally confirmed that MnO is an insulator and its resistivity is only 10^{17} Ω·cm at room temperature. The same problem has been encountered when using energy band theory to explain the conductive properties of other transition metal oxides such as CoO, Fe_2O_3 and CuO. So far, the mechanism of conductivity of oxide semiconductor materials can be summarized into two types, namely, narrow-band theory and polariton theory.

2.1. *Narrow-band theory*

The narrow-band theory was first proposed by Nevill Mott in 1949.[37] He believed that transition metal crystals become insulators when the atomic spacing is so large that carriers cannot transfer to each other. From the energy band theory, the energy band becomes wider as the distance between isolated atoms becomes smaller, and conversely, the energy band becomes narrower as the distance between isolated atoms becomes larger. Therefore, in a crystalline material with an unfilled valence band, the energy band is narrow enough to obtain a material with insulator properties. For transition metal crystals, the energy bandwidth of the d-band is about a few electron volts, so the conductive process can proceed smoothly. However, for transition metal oxide crystals, the large distance between transition metal cations leads to the poor commonality between electrons, increasing the effective mass of carriers and making it difficult for the conductive process to occur. Therefore, transition metal oxides exhibit insulator properties at room temperature.[38,39]

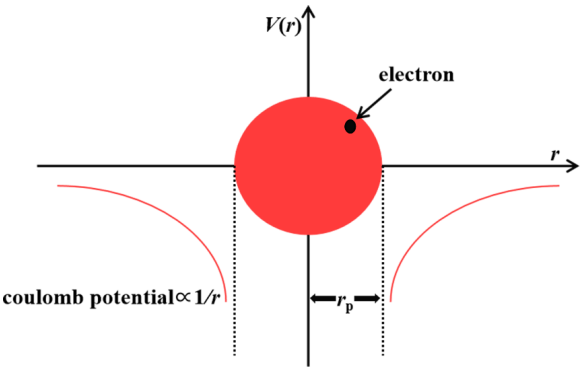

Fig. 1. Polaron model.

2.2. *Polariton theory*

The concept of polariton was first introduced by the Soviet physicist Lev Davidovich Landau in 1933 (Fig. 1).[40] Subsequently, the British physicists Nevill Mott and Rudolf Peierls also explored the polariton theory, as the single-electron approximation in the energy band theory failed to reasonably explain the conductive properties of transition metal oxides.[37] They proposed that since the ion is charged in ionic crystals, it can interact with carriers to produce polarization phenomena. The carriers are trapped by this polarized medium, which is called carrier self-trapping. The carriers and carrier-ion interactions can be considered as a whole, and the whole is called the polarizer. If the overlap of electron clouds between ions is large, the energy band is wide and the corresponding degree of lattice distortion is large it is called a large polariton. On the contrary, when the electron cloud overlap is small and the polarization radius is smaller than the lattice constant, it is called a small polariton (e.g., NiO, the polarization radius is about 1 Å and the spacing between Ni^{2+} ions is about 3 Å, so it is a small polariton). The energy level of the polariton is located near the bottom of the conduction band or the top of the valence band. When polaritons are thermally excited, the carriers will jump from one atom to another. Polariton theory suggests that the conductive process of transition metal oxides is conducted by carriers jumping between adjacent energy levels, rather than through carrier motion in the energy band. Thus, this mechanism of conductivity is called the hopping conductivity model.[41–43]

3. Factors for the Formation of Single-Phase Multi-Component Oxides

The HEO with multiple elements make it difficult to synthesize polycrystalline ceramics with a single crystal structure.

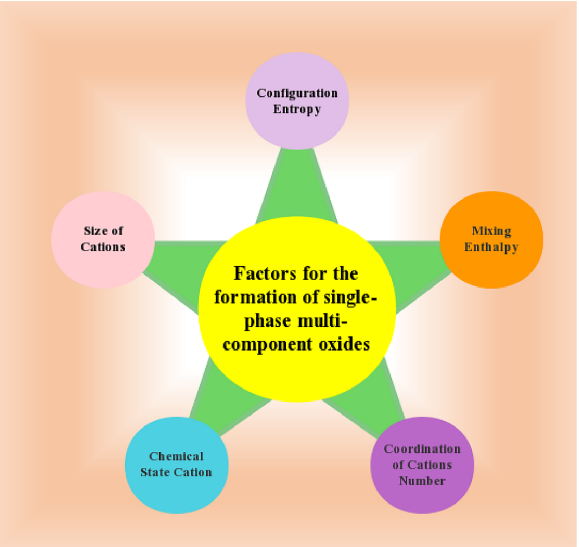

Fig. 2. Parameters affecting the formation of single-phase multi-component oxides.

It is necessary to consider various factors affecting the formation of single phase of HEO to make them exhibit a single-phase structure. The main factors of single-phase formation are described in Fig. 2, which include conformational entropy, enthalpy change of mixing, ionic radius, chemical valence and cation coordination number (CN). A brief analysis of the factors other than the conformational entropy is discussed.

(1) Enthalpy of mixing (ΔH_{mix})
For some metal oxides with high solubility, this is not beneficial for the formation of single-phase polytropic oxides due to their usually large negative values of mixing enthalpy (ΔH_{mix}) and offsetting values of mixing entropy. Metal oxides with different structures usually have larger positive values of mixing enthalpy (ΔH_{mix}) and so they cannot be compensated by high entropy effects alone. We can take advantage of the fact that higher reaction temperatures can lead to phase changes and mixing. From the perspective of mixing enthalpy change, the preparation of single-phase high-entropy oxides should be based on the oxides with different crystal structures, i.e., at least one oxide should have a different crystal structure compared to the other oxides when selecting the initial oxide raw material.[44,45]

(2) Size of cations
The cation radius is also a key factor affecting the formation of single-phase high-entropy oxides. When selecting raw materials for the initial oxide, metal oxides with similar cation radii should be selected as much as possible for the material preparation.

(3) Chemical valence states
For single-phase high-entropy oxides, the heterovalent metal cations occupy the same cationic sublattice sites, while the anions remain electrically neutral in the lattice.[46,47] Therefore, the propensity of the constituent elements for a specific chemical valence state plays a key role in the formation of single-phase high-entropy oxides. For example, to synthesize a high-entropy oxide with a single rock salt phase structure, a metal oxide with +2 valence or a tendency to form +2 valence during sintering should be selected. Therefore, it is crucial that the metal cations exhibit specific chemical valence states under different sintering conditions.[48]

(4) Cation coordination number
In the crystal structure of ionic crystals, each ion is surrounded by other anions or cations. The number of ions closely surrounding a particular ion is the CN, which depends on the relative size of the ions. All cations occupying the same sublattice have the same CN, e.g., four coordination in a tetrahedral sublattice and six coordination in an octahedral sublattice in a spinel structure. Hence, cations with the same CN should be used for the preparation of HEO.[49–51]

4. Electrical Properties

HEO exhibit high conformational entropy and stable crystal structures under the combined effect of multiple metal cations.[52–56] They can significantly impact the electrical properties of oxide ceramics. The subject has been studied in various publications and the following discussion will focus on electrical conductivity, dielectric properties and piezoelectric properties.

4.1. *Electrical conductivity*

The distorted structure and high electron scattering of high-entropy oxide materials reduce the electrical conductivity,[57] so the low conductivity of high-entropy oxide materials offers new opportunities for the fabrication of thin-film insulators. Owing to the high stability of the crystal structure, the high-entropy ceramics possess stable negative temperature coefficient (NTC) and aging properties, making them promising thermistor materials. The major discoveries concerning the conductivity of oxides are reviewed.

Tsau *et al.*[58] fabricated different thin film oxides as $Ti_xFeCoNi$ ($x = 0$, 0.25, 0.5, 0.75 and 1), $TiFeCoNiCu_x$ ($x = 1$, 2 and 3) and $Al_xCrFeCoNiCu$ ($x = 0.5$ and 1) by magnetron sputtering and studied their resistivities. The resistivities of these high-entropy alloy oxides are about 30 $\mu\Omega\cdot$cm for $Ti_xFeCoNi$ oxide films, about 100 $\mu\Omega\cdot$cm for $TiFeCoNiCu_3$ oxide films, and about 650 $\mu\Omega\cdot$cm for $Al_{0.5}CrFeCoNiCu$ oxide films. Their room-temperature resistivity are close to that of most of the metallic alloys, and lower than that of RuO_2 single crystal, also much lower than that of ITO. The electrical resistivities of these alloy oxide thin films were dominated by the compositions and oxygen-content.

$(AlCrTaTiZr)O_x$ thin films were deposited by Lin *et al.*[59] using DC magnetron sputtering in different concentrations of

oxygen. The resistivity of $(AlCrTaTiZr)O_x$ films was investigated. The results showed an increase with increasing oxygen concentration, reaching 10^{12} $\mu\Omega \cdot$cm.

Gild *et al.*[60] studied the conductivity of eight fluorite HEO. A lower conductivity than Y_2O_3-stabilized ZrO_2 was shown for all samples. In addition, they pointed to the fact that the addition of CaO to the blast furnace decreases the conductivity at low temperatures. Since the conductivity is influenced by grain size and grain boundary resistance, they concluded that the small grain size of fluorite is the major reason for the reduction in conductivity.

Balcerzak *et al.*[61] studied the conductivity of HEO (Co, Cu, Mg, Ni, Zn)O. The results showed that the variation of conductivity with temperature follows an Arrhenius-type curve. The highest activation energy, which was equal to 1.01 eV, was observed for the lowest temperature range (478–641 K), whereas the lowest value of 0.62 eV was determined for the temperature range of 990–1148 K. The highest electrical conductivity of the (Co, Cu, Mg, Ni, Zn)O high-entropy oxide was measured at 1148 K, and it was equal to 8.03×10^{-2} S cm^{-1}.

Wang *et al.*[62] successfully fabricated an entropy stabilized $(Co_{0.2}Mn_{0.2}Fe_{0.2}Zn_{0.2}Ni_{0.2})_3O_4$ ceramic. The prepared ceramic obtained exceptional NTC properties between −75°C and 75°C (Fig. 3(a)). Most importantly, the prepared ESO exhibits excellent aging stability, i.e., the aging coefficient ($\Delta R/R_0$) can reach 0.19% under accelerated aging conditions at 125°C for 600 h (Fig. 3(b)). It is indicated that the enhanced aging stability comes from the disordered distribution of cations in the spinel sublattice.

Zheng *et al.*[63] synthesized $(Ca_{0.5}Ce_{0.5})(Nb_{0.25}Ta_{0.25}Mo_{0.25}W_{0.25})O_4$ scheelite phase high entropy ceramics and analyzed their high-temperature NTC properties. The effect of the high entropy is also discussed on its internal structure and electrical properties (Figs. 3(c) and 3(d)). The high entropy effect imparts a great disordered lattice to the ceramics, which limits the diffusion of ions.

4.2. *Dielectric properties*

The dielectric properties are essential characteristics for designing electronic devices, such as capacitors for energy storage.[64] A lot of studies have shown that high entropy oxide materials with rock salt structures have high dielectric constants. Besides, their properties can be improved by varying the concentration

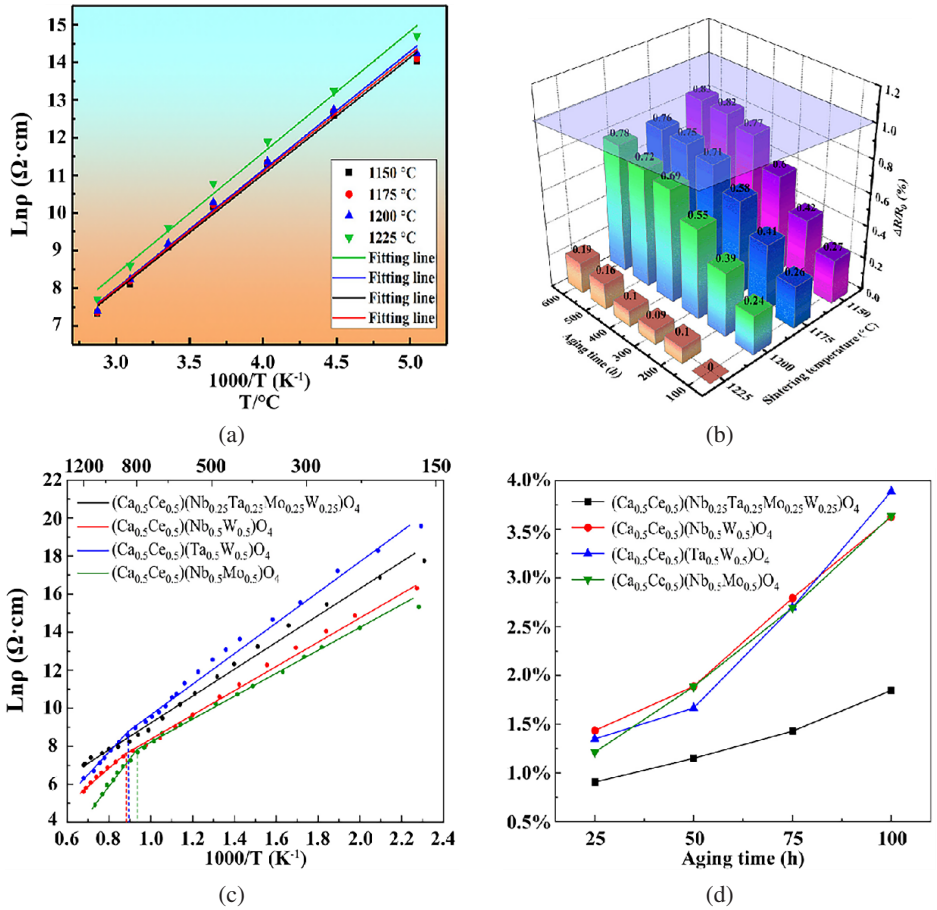

Fig. 3. (a) Plots of the Ln(ρ) versus 1000/T relation and (b) aging drift $\Delta R/R_0$ at different aging times of $(Co_{0.2}Mn_{0.2}Fe_{0.2}Zn_{0.2}Ni_{0.2})_3O_4$ ceramics sintered at different temperatures: 1150, 1175, 1200 and 1225°C[62]; (c) plots of the Ln(ρ) versus 1000/T relation and (d) aging drift $\Delta R/R_0$ at different aging times of high-entropy scheelite ceramics and conventional scheelite ceramics sintered at 1300°C.[63]

of constituent elements, which indicates a promising application of high-entropy oxide materials in capacitor-based energy storage devices.[65] Other structures of HEO are being tried to be developed for energy storage, such as perovskites.

The large dielectric constants were observed in HEO with rock salt structure by Bérandan *et al*.[65] The dielectric constant (relative permittivity) of $(Mg,Co,Ni,Cu,Zn)_{0.95}Li_{0.05}O$ was close to 2×10^5 measured by the LCR bridge at 440 K and 20 Hz. For the (Mg,Co,Ni,Cu,Zn)O family, large values of dielectric constant are obtained as long as a high-entropy oxide phase is formed, regardless of the substitution. For example, high entropy (Mg,Co,Ni,Cu,Zn)O without any substitution has a dielectric constant greater than 1000, while the dielectric loss ($\tan\delta$) was measured below 0.01 in the range of 313 K and 1 MHz.

Zhou *et al*.[66] prepared high entropy perovskites $Ba(Zr_{0.2}Ti_{0.2}Sn_{0.2}Hf_{0.2}Me_{0.2})O_3$ (Me=Nb^{5+}, Ta^{5+}). Their dielectric properties were investigated and it was found that the dielectric constant and dielectric loss decreased slowly with the increase of frequency from 1 to 1000 kHz. In addition, the dielectric constant and dielectric loss have high stability at fixed frequencies at temperatures from 303 to 473 K. At frequencies from 1 to 1000 kHz, the dielectric constants of $Ba(Zr_{0.2}Ti_{0.2}Sn_{0.2}Hf_{0.2}Ta_{0.2})O_3$ and $Ba(Zr_{0.2}Ti_{0.2}Sn_{0.2}Hf_{0.2}Nb_{0.2})O_3$ are in the range of 90–113 and 120–140, respectively, which are attributed to the small concentration of titanium in the B-site sublattice and the small grain size. It is intriguing to note that the dielectric loss ($\tan\delta$) is below 0.002 in the frequency range of 20–2 Hz. They mentioned that it can be inferred that entropic stability contributes to the stability of the permittivity loss tangent owing to the high entropy improving the thermal and electrochemical stability.[67,68] The permittivity of this material is very low despite the superior permittivity stability (Figs. 4(a) and 4(b)). Also, these materials display high resistivity and moderate breakdown strength (290–370 kV/cm), which is attributed to the effective contribution of the configuration entropy in enhancing charge carrier scattering.

The material $(Na_{0.2}Bi_{0.2}Ba_{0.2}Sr_{0.2}Ca_{0.2})TiO_3$ with a high configuration entropy was synthesized using a solid-state method by Pu *et al*.[69] The calculations of thermodynamic parameters and relevant experiments revealed that both entropy and enthalpy could drive the formation of stable systems. For the study of the dielectric properties, the diffuse phase transport and frequency dispersion with an energy density of 1.02 J cm^{-3} were shown at 145 kV cm^{-1}.

Du *et al*.[70] successfully synthesized $Ba(Ti_{1/6}Sn_{1/6}Zr_{1/6}Hf_{1/6}Nb_{1/6}Ga_{1/6})O_3$, a high entropy ceramic (HECs) with perovskite structure, using a solid-state reaction method. Its dielectric properties were investigated and the dielectric constant was found to be 40–75 below 1 MHz, with a dielectric loss tangent around 0.15 (Figs. 4(c) and 4(d)). The findings revealed the dielectric relaxation behavior of the high-entropy perovskite ceramics.

Radon *et al*.[71] prepared the synthesis of high entropy (Zn, Mg, Ni, Fe, Cd) Fe_2O_4 ferrite using a co-precipitation

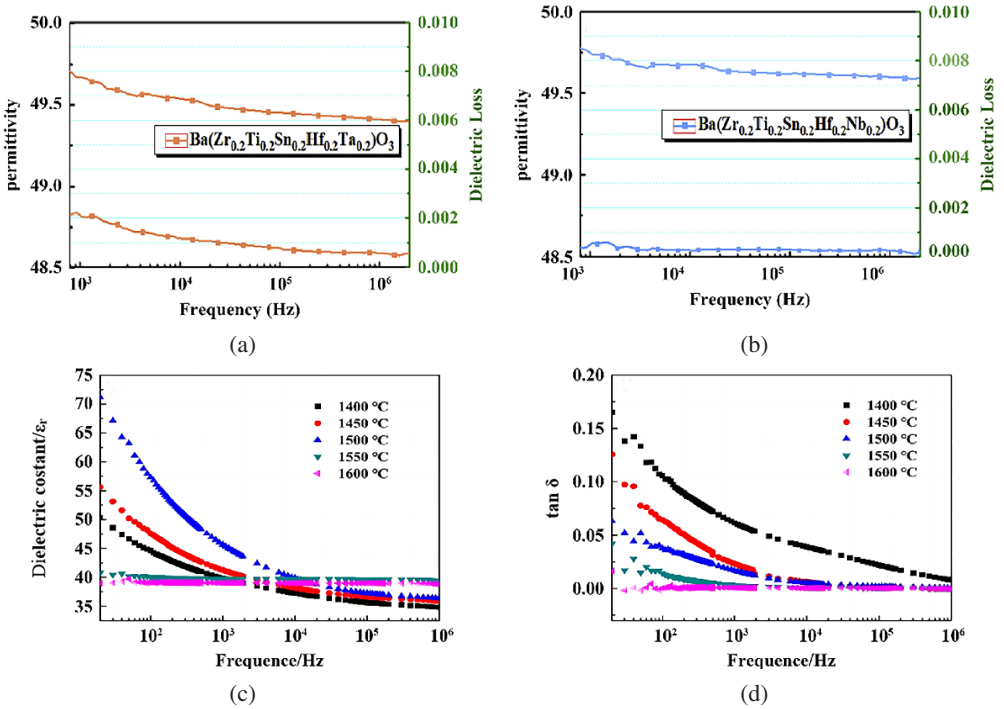

Fig. 4. Relative permittivity (left axis) and dielectric loss (right axis) versus frequency for (a) $Ba(Zr_{0.2}Ti_{0.2}Sn_{0.2}Hf_{0.2}Ta_{0.2})O_3$ at room temperature[67]; (b) $Ba(Zr_{0.2}Ti_{0.2}Sn_{0.2}Hf_{0.2}Nb_{0.2})O_3$ at room temperature[67]; (c) a Dielectric constant ε_r and (d) dielectric loss tan δ as function of frequency of $Ba(Ti_{1/6}Sn_{1/6}Zr_{1/6}Hf_{1/6}Nb_{1/6}Ga_{1/6})O_3$ ceramics sintered at different temperatures.[70]

method. They found that the high-frequency composite dielectric constant is affected by temperature and frequency, with values comparable to the commercial $BaTiO_3$. The highest microwave absorption (RL < −25 dB and SE < −50 dB) was obtained at 1.9–2.1 GHz with a material layer of 0.8–1 cm thickness. The low values of the real part of the magnetic permeability and the high values of the magnetic loss in the high-frequency region may be related to grain boundaries, chemical inhomogeneities and small particle size. In addition, they found that the high-frequency short-range mobility of this material is associated with the tunneling of electrons between Fe^{2+} and Fe^{3+} ions, while the long-range mobility is linked to the diffusion of charge carriers through the grain boundaries.

The single-phase perovskite $Na_{0.30}K_{0.07}Ca_{0.24}La_{0.18}Ce_{0.21}TiO_3$ was prepared by Vinnik *et al*.,[72] as well as its dielectric properties were tested. The loss angle tangent of $BaTiO_3$ was found to be significantly smaller than that of HEO. In addition, there was a significant difference in the thermal behavior of tanδ between $Na_{0.30}K_{0.07}Ca_{0.24}La_{0.18}Ce_{0.21}TiO_3$ and $BaTiO_3$. For HEO, the loss angle tangent grows above 300°C, but for $BaTiO_3$, the tanδ versus T curve shows a single maximum at all frequencies of the probe voltage.

4.3. *Piezoelectric properties*

Piezoelectric materials are perovskite structures based on lead zirconate titanate ($PbTiO_3$) used commonly in transducers, other sensors and actuators, etc.[73] However, the toxic Pb can cause environmental pollution. Additionally, the high vapor pressure of the sintering process is an additional problem for these materials. Researchers have tried to synthesize high-entropy oxides with good piezoelectric properties as alternatives to lead zirconate titanate, as described below.

The lead-free piezoelectric ceramic system with perovskite structure $(Bi_{1-x-y}Na_{0.925-xy}Li_{0.075})_{0.5}Ba_xSr_yTiO_3$ was prepared by Lin *et al*.[73] and its piezoelectric and ferroelectric properties were investigated. It was confirmed that better piezoelectric coefficients were obtained by numerical comparison with $Bi_{0.5}Na_{0.5}TiO_3$. For ceramics with compositions close to MPB (x = 0.04–0.08 and y = 0.02–0.04), the piezoelectric coefficient d_{33} = 133–193 pC/N and the planar electromechanical coupling coefficient k_P = 16.2–32.1%.

The $Pb_{0.94}Sr_{0.06}(Zr_{0.50}Ti_{0.50})_{0.99}Cr_{0.01}O_3$ was prepared by Zachariasz *et al*.[74] using the solid-phase method. It was found that the obtained ceramics are ferroelectric hard materials, which is why it can be used for the construction of resonators, filters and ultrasonic sensors. Moreover, this material exhibits high stability of the relative variation of the resonant frequency $\Delta f_r/f_r$ and well stability of the piezoelectric parameters. The d_{33} component of its piezoelectric coefficient is 68 pC/N.

Bochenek *et al*.[75] synthesized $(Zr_{0.49}Ti_{0.51})_{0.94}Mn_{0.014}Sb_{0.02}W_{0.014}Ni_{0.02}O_3$ ceramics with a perovskite structure. Their results revealed that the materials have a high piezoelectric coefficient of d_{33} = 278 pC/N. In addition, the materials have a low dielectric loss at both room and phase transition temperatures. Moreover, their properties (high values of piezoelectric parameters and small dielectric losses) make the material suitable for modern micromechanical electronics applications.

A strategy for introducing anisotropic phases in high entropy perovskites to obtain ferroelectricity was proposed by Li *et al*.[76] $(1-x)Pb(Mg_{0.2}Zn_{0.2}Nb_{0.2}Ta_{0.2}W_{0.2})O_3$-$xPbTiO_3$ was used as a model system to demonstrate the feasibility of this concept. The MPB structure was formed in the composition range of x=0.275–0.35, and ferroelectric and piezoelectric properties were obtained. The d_{33} reaches a maximum at x=0.325 (d_{33}=92.4 pC/N), which is owing to the increase of the polarization direction introduced by the coexistence of pseudocubic and tetragonal phases as the composition is in the MPB interval.

5. Conclusions and Outlook

In the past few years, scholars have done a lot of research in the field of electrical properties of high-entropy oxides. So far, it can be said that the main electrical features of HEO are largely different from those of conventional oxides, such as low electrical conductivity, stable aging properties and huge dielectric constants. The high-entropy oxides have advantages in terms of stable structure, lattice distortion and degree of disorder. It implies a great chance to find efficient insulating, semiconductor materials in high-entropy oxide. In addition, most of the results reveal that the high-entropy oxides exhibit electrical features covering the electrical states from the parent oxide, which are different from the conventional doped oxides. Based on these obvious differences, we propose directions for future research.

Firstly, the properties of HEO can be tailored by compositional design, but the role of individual elements in certain applications and their relationship to cocktail effects are not understood. Currently, studies of HEO are in an early stage and it seems that "customization" is mostly done in a stochastic way. Therefore, it is highly significant to be able to design HEO rationally. An effective approach is to choose a basic model with new elements gradually added or replaced to modify the configurational entropy of the system.

Secondly, starting from the concept of high entropy itself, it is no longer limited to the synthesis of oxides with five major elements in equal or nearly equal proportions. A comparative study of high-entropy materials and corresponding medium or low-entropy materials is performed by extracting one or more elements from a system. Such research is expected to provide a more sophisticated understanding of the concept of high entropy. Of course, comparisons between properties and reaction mechanisms are essential.

Acknowledgments

This work was financially supported by the National Natural Science Foundation of China under No. 61971094, Natural Science Foundation of Sichuan Province under Nos. 2022NSFSC0485 and 2022NSFSC0870.

Declaration of Interest Statement

The authors declare that they have no known competing financial interests or personal relationships that could have appeared to influence the work reported in this paper.

References

[1]D. B. Miracle, High entropy alloys as a bold step forward in alloy development, *Nat. Commun*. **10**, 1805 (2019).
[2]J. W. Yeh, S. K. Chen, S. J. Lin, J. Y. Gan, T. S. Chin, T. T. Shun, C. H. Tsau and S. Y. Chang, Nanostructured high-entropy alloys with multiple principle elements: Novel alloy design concepts and outcomes, *Adv. Eng. Mater*. **6**, 299 (2004).
[3]S. J. McCormack and A. Navrotsky, Thermodynamics of high entropy oxides, *Acta Mater*. **202**, 1 (2021).
[4]S. Zhou, Y. Pu, X. Zhang, Y. Shi, Z. Gao, Y. Feng, G. Shen, X. Wang and D. Wang, High energy density, temperature stable lead-free ceramics by introducing high entropy perovskite oxide, *Chem. Eng. J*. **427**, 131684 (2022).
[5]A. J. Wright, Q. Y. Wang, C. Z. Hu, Y. T. Yeh, R. K. Chen and J. Luo, Single-phase duodenary high-entropy fluorite/pyrochlore oxides with an order-disorder transition, *Acta Mater*. **211**, 116858 (2021).
[6]A. Sarkar, R. Djenadic, N. J. Usharani, K. P. Sanghvi, V. S. K. Chakravadhanula, A. S. Gandhi, H. Hahn and S. S. Bhattacharya, Nanocrystalline multicomponent entropy stabilised transition metal oxides, *J. Eur. Ceram. Soc*. **37**, 747 (2017).
[7]B. Cantor, I. T. H. Chang, P. Knight and A. J. B. Vincent, Microstructural development in equiatomic multicomponent alloys, *Mater. Sci. Eng. A* **375–377**, 213 (2004).
[8]R. Feng, P. K. Liaw, M. C. Gao and M. Widom, First-principles prediction of high-entropy-alloy stability, *npj Comput. Mater*. **3**, 50 (2017).
[9]M. C. Gao, G. Pan, J. A. Hawk, L. Z. Ouyang, D. E. Alman and M. Widom, Computational modeling of high-entropy alloys: Structures, thermodynamics and elasticity, *J. Mater. Res*. **32**, 3627 (2017).
[10]M. Widom, Modeling the structure and thermodynamics of high-entropy alloys, *J. Mater. Res*. **33**, 2881 (2018).
[11]E. P. George, D. Raabe and R. O. Ritchie, High-entropy alloys, *Nat. Rev. Mater*. **4**, 515 (2019).
[12]D. Bérardan, A. Meena, S. Franger, C. Herrero and N. Dragoe, Controlled Jahn-Teller distortion in (MgCoNiCuZn)O-based high entropy oxides, *J. Alloys. Compd*. **704**, 693 (2017).
[13]C. M. Rost, Z. Rak, D. W. Brenner and J. P. Maria, Local structure of the $Mg_xNi_xCo_xCu_xZn_xO$(x = 0.2) entropy-stabilized oxide: An EXAFS study, *J. Am. Ceram. Soc*. **100**, 2732 (2017).
[14]R. Djenadic, A. Sarkar, O. Clemens, C. Loho, M. Botros, V. S. K. Chakravadhanula, C. Kübel, S. S. Bhattacharya, A. S. Gandhi and H. Hahn, Multicomponent equiatomic rare earth oxides, *Mater. Res. Lett*. **5**, 102 (2017).
[15]K. P. Tseng, Q. Yang, S. J. McCormack and W. M. Kriven, High-entropy, phase-constrained, lanthanide sesquioxide, *J. Am. Ceram. Soc*. **103**, 569 (2020).
[16]B. Jiang, Y. Yu, J. Cui, X. Liu, L. Xie, J. Liao, Q. Zhang, Y. Huang, S. Ning, B. Jia, B. Zhu, S. Bai, L. Chen, S. J. Pennycook and J. He, High-entropy-stabilized chalcogenides with high thermoelectric performance, *Science* **371**, 830 (2021).
[17]A. J. Wright, Q. Wang, S. T. Ko, K. M. Chung, R. Chen and J. Luo, Size disorder as a descriptor for predicting reduced thermal conductivity in medium- and high-entropy pyrochlore oxides, *Scr. Mater*. **181**, 76 (2020).
[18]T. Y. Chen, S. Y. Wang, C. H. Kuo, S. C. Huang, M. H. Lin, C. H. Li, H. Y. T. Chen, C. C. Wang, Y. F. Liao, C. C. Lin, Y. M. Chang, J. W. Yeh, S. J. Lin, T. Y. Chen and H. Y. Chen, In operando synchrotron X-ray studies of a novel spinel $(Ni_{0.2}Co_{0.2}Mn_{0.2}Fe_{0.2}Ti_{0.2})_3O_4$ high-entropy oxide for energy storage applications, *J. Mater. Chem. A* **8**, 21756 (2020).
[19]M. Fracchia, M. Manzoli, U. Anselmi-Tamburini and P. Ghigna, A new eight-cation inverse high entropy spinel with large configurational entropy in both tetrahedral and octahedral sites: Synthesis and cation distribution by X-ray absorption spectroscopy, *Scr. Mater*. **188**, 26 (2020).
[20]S. Marik, D. Singh, B. Gonano, F. Veillon, D. Pelloquin and Y. Bréard, Enhanced magnetic frustration in a new high entropy diamond lattice spinel oxide, *Scr. Mater*. **186**, 366 (2020).
[21]Z. F. Zhao, H. Chen, H. M. Xiang, F. Z. Dai, X. H. Wang, W. Xu, K. Sun, Z. J. Peng and Y. C. Zhou, High-entropy $(Y_{0.2}Nd_{0.2}Sm_{0.2}Eu_{0.2}Er_{0.2})AlO_3$: A promising thermal/environmental barrier material for oxide/oxide composites, *J. Mater. Sci. Technol*. **47**, 45 (2020).
[22]Z. F. Zhao, H. M. Xiang, F. Z. Dai, Z. J. Peng and Y. C. Zhou, $(La_{0.2}Ce_{0.2}Nd_{0.2}Sm_{0.2}Eu_{0.2})_2Zr_2O_7$: A novel high-entropy ceramic with low thermal conductivity and sluggish grain growth rate, *J. Mater. Sci. Technol*. **35**, 2647 (2019).
[23]J. L. Braun, C. M. Rost, M. Lim, A. Giri, D. H. Olson, G. N. Kotsonis, G. Stan, D. W. Brenner, J. P. Maria and P. E. Hopkins, Charge-induced disorder controls the thermal conductivity of entropystabilized oxides, *Adv. Mater*. **30**, 1805004 (2018).
[24]S. Zhai, J. Rojas, N. Ahlborg, K. Lim, M. F. Toney, H. Jin, W. C. Chueh and A. Majumdar, The use of poly-cation oxides to lower the temperature of two-step thermochemical water splitting, *Energy. Environ. Sci*. **11**, 2172 (2018).
[25]Z. Y. Ding, J. J. Bian, S. Shuang, X. D. Liu, Y. C. Hu, C. W. Sun and Y. Yang, High entropy intermetallic-oxide core-shell nanostructure as superb oxygen evolution reaction catalyst, *Adv. Sustain. Syst*. **4**, 1900105 (2020).
[26]Y. Zhang, T. Lu, Y. K. Ye, W. J. Dai, Y. A. Zhu and Y. Pan, Stabilizing oxygen vacancy in entropy-engineered $CoFe_2O_4$-type catalysts for co-prosperity of efficiency and stability in an oxygen evolution reaction, *ACS Appl. Mater. Interfaces* **12**, 32548 (2020).
[27]T. Wang, H. Chen, Z. Z. Yang, J. Y. Liang and D. Sheng, High-entropy perovskite fluorides: A new platform for oxygen evolution catalysis. *J. Am. Chem. Soc*. **142**, 4550 (2020).
[28]J. H. Yan, D. Wang, X. Y. Zhang, J. S. Li, Q. Du, X. Y. Liu, J. R. Zhang and X. W. Qi, A high-entropy perovskite titanate lithium-ion battery anode, *J. Mater. Sci*. **55**, 6942 (2020).
[29]H. Chen, N. Qiu, B. Wu, Z. M. Yang, S. Sun and Y. Wang, A new spinel high-entropy oxide $(Mg_{0.2}Ti_{0.2}Zn_{0.2}Cu_{0.2}Fe_{0.2})_3O_4$ with fast reaction kinetics and excellent stability as an anode material for lithium ion batterie, *RSC Adv*. **10**, 9736 (2020).
[30]Q. S. Wang, A. Sarkar, D. Wang, L. Velasco, R. Azmi, S. S. Bhattacharya, T. Bergfeldt, A. Düvel, P. Heitjans, T. Brezesinski, H. Hahn and B. Breitung, Multi-anionic and -cationic compounds: New high entropy materials for advanced Li-ion batteries, *Energy. Environ. Sci*. **12**, 2433 (2019).
[31]Z. Y. Lun, B. Ouyang, D.-H. Kwon, Y. Ha, E. E. Foley, T.-Y. Huang, Z. Cai, H. Kim, M. Balasubramanian, Y. Z. Sun, J. P. Huang, Y. S. Tian, H. Kim, B. D. McCloskey, W. L. Yang, R. J. Clément, H. W. Ji and G. Ceder, Cation-disordered rocksalt-type high-entropy cathodes for Li-ion batteries, *Nat. Mater*. **20**, 214 (2021).

[32]B. Zhao, Z. K. Yan, Y. Q. Du, L. J. Rao, G. Y. Chen, Y. Y. Wu, L. T. Yang, J. C. Zhang, L. M. Wu, D. W. Zhang and R. C. Che, High-entropy enhanced microwave attenuation in titanate perovskites, *Adv. Mater*. **35**, 2210243 (2023).
[33]M. Kheradmandfard, H. Minouei, N. Tsvetkov, A. K. Vayghan, S. F. Kashani-Bozorg, G. Kim, S. I. Hong and D.-E. Kim, Ultrafast green microwave-assisted synthesis of high-entropy oxide nano-particles for Li-ion battery applications, *Mater. Chem. Phys*. **262**, 124265 (2021).
[34]D. Wang, S. D. Jiang, C. Q. Duan, J. Mao, Y. Dong, K. Z. Dong, Z. Y. Wang, S. H. Luo, Y. G. Liu and X. W. Qi, Spinel-structured high entropy oxide $(FeCoNiCrMn)_3O_4$ as anode towards superior lithium storage performance, *J. Alloys. Compd*. **844**, 156158 (2020).
[35]D. Adler, Electrical and optical properties of transition-metal oxides, *Radiat. Eff. Defects Solids*. **4**, 123 (1970).
[36]S. Walia, S. Balendhran, H. Nili, S. Zhuiykov, G. Rosengarten, Q. H. Wang, M. Bhaskaran, S. Sriram, M. S. Strano and K. Kalantar-zade, Transition metal oxides–thermoelectric properties, *Prog. Mater. Sci*. **58**, 1443 (2013).
[37]N. F. Mott, The basis of the electron theory of metals, with special reference to the transition metals, *Proc. Phys. Soc. A* **62**, 416 (1949).
[38]L. C. Fan, J. C. Yao, P. Huo, B. Wang, Z. J. Liu, A. M. Chang and J. H. Wang, Design and synthesis of thermistor materials with high aging stability: Multicomponent equiatomic Mn-Co-Ni-Al-Zn-O ceramics, *Mater. Sci. Semicond. Process*. **155**, 107263 (2023).
[39]A. Feteira, Negative temperature coefficient resistance (NTCR) ceramic thermistors: An industrial perspective, *J. Am. Ceram. Soc*. **92**, 967 (2009).
[40]C. J. G. M. Langerak, J. Singleton, J. A. A. J. Perenboom, F. M. Peeters, J. T. Devreese, D. J. Barnes, R. J. Nicholas, S. Huant, J. J. Harris, C. T. Foxon and B. Etienne, Far-infrared magneto-optical studies of the polaron effect in low dimensional GaAs-(Ga, Al)As structures, *Phys. Scr*. **T39**, 308 (1991).
[41]A. J. Bosman and C. Crevecoeur, Mechanism of the electrical conduction in Li-doped NiO, *Phys. Rev*. **144**, 763 (1966).
[42]R. D. Shannon, Dielectric polarizabilities of ions in oxides and fluorides, *J. Appl. Phys*. **73**, 348 (1993).
[43]B. F. Levine, Bond susceptibilities and ionicities in complex crystal structures, *J. Chem. Phys*. **59**, 1463 (1973).
[44]C. M. Rost, E. Sachet, T. Borman, A. Moballegh, E. C. Dickey, D. Hou, J. L. Jones, S. Curtarolo and J. Maria, Entropy stabilized oxides, *Nat. Commun*. **6**, 1 (2015).
[45]G. Anand, A. P. Wynn, C. M. Handley and C. L. Freeman, Acta materialia phase stability and distortion in high-entropy oxides, *Acta Mater*. **146**, 119 (2018).
[46]A. Sarkar, R. Djenadic, D. Wang, C. Hein, R. Kautenburger, O. Clemens and H. Hahn, Rare earth and transition metal based entropy stabilised perovskite type oxides, *J. Eur. Ceram. Soc*. **38**, 2318 (2018).
[47]S. Jiang, T. Hu, J. Gild, N. Zhou, J. Nie, M. Qin, T. Harrington, K. Vecchio and J. Luo, A new class of high-entropy perovskite oxides, *Scr. Mater*. **142**, 116 (2018).
[48]A. Sarkar, Q. Wang, A. Schiele, M. R. Chellali, S. S. Bhattacharya, D. Wang, T. Brezesinski, H. Hahn, L. Velasco and B. Breitung, High-entropy oxides: Fundamental aspects and electrochemical properties, *Adv. Mater*. **31**, 1806236 (2019).
[49]S. Guillemet-Fritsch, J. L. Baudour, C. Chanel, F. Bouree and A. Rousset, X-ray and neutron diffraction studies on nickel zinc manganite $Mn_{2.35-x}Ni_{0.65}Zn_xO_4$ powders, *Solid. State. Ion*. **132**, 63 (2000).
[50]K. Krezhov and P. Konstantinov, Cationic distributions in the binary oxide spinels $MxCo_{3-x}O_4$ (M = Mg, Cu, Zn, Ni), *Phys. B* **236**, 157 (1997).
[51]N. Okasha, Structural characterization and magnetic properties of $Zn_{1-x}Cu_xCr_{0.8}Fe_{1.2}O_4$; $0.1 \le x \le 0.9$, *Mater. Chem. Phys*. **84**, 63 (2004).
[52]J. Dąbrowa, M. Stygar, A Mikuła, A. Knapik, K. Mroczka, W. Tejchman, M. Danielewski and M. Martin, Synthesis and microstructure of the $(Co, Cr, Fe, Mn, Ni)_3O_4$ high entropy oxide characterized by spinel structure, *Mater. Lett*. **216**, 32 (2018).
[53]M. Biesuz, S. Fu, J. Dong, A. N. Jiang, D. Y. Ke, Q. Xu, D. G. Zhu, M. Bortolotti, M. J. Reece, C. F. Hu and S. Grasso, High entropy $Sr(Zr_{0.94}Y_{0.06})_{0.2}$ $Sn_{0.2}Ti_{0.2}Hf_{0.2}Mn_{0.2})O_{3-x}$ perovskite synthesis by reactive spark plasma sintering, *J. Asian Ceram. Soc*. **7**, 127 (2019).
[54]H. Chen, Z. F. Zhao, H. M. Xiang, F. Z. Dai, W. Xu, K. Sun, J. C. Liu and Y. C. Zhou, High entropy $(Y_{0.2}Yb_{0.2}Lu_{0.2}Eu_{0.2}Er_{0.2})_3Al_5O_{12}$: A novel high temperature stable thermal barrier material, *J. Mater. Sci. Technol*. **48**, 57 (2020).
[55]F. Vayer, C. Decorse, D. Bérardan and N. Dragoe, New entropy-stabilized oxide with pyrochlore structure: $Dy_2(Ti_{0.2}Zr_{0.2}Hf_{0.2}Ge_{0.2}Sn_{0.2})_2O_7$, *J. Alloys. Compd*. **883**, 1 (2021).
[56]T. X. Nguyen, J. Patra, J. K. Chang and J. M. Ting, High entropy spinel oxide nanoparticles for superior lithiation-delithiation performance, *J. Mater. Chem. A* **8**, 18963 (2020).
[57]X. J. Chen, K. A. Khor, S. H. Chan and L. G. Yu, Influence of microstructure on the ionic conductivity of yttria-stabilized zirconia electrolyte, *Mater. Sci. Eng. A* **335**, 246 (2002).
[58]C. H. Tsau, Y. C. Yang, C. C. Lee, L. Y. Wu and H. J. Huang, The low electrical resistivity of the high-entropy alloy oxide thin films, *Procedia Eng*. **36**, 246 (2012).
[59]M. I. Lin, M. H. Tsai, W. J. Shen and J. W. Yeh, Evolution of structure and properties of multi-component $(AlCrTaTiZr)O_x$ films, *Thin Solid Films* **518**, 2732 (2010).
[60]J. Gild, M. Samiee, J. L. Braun, T. Harrington, H. Vega, P. E. Hopkins, K. Vecchio and J. Luo, High-entropy fluorite oxides, *J. Eur. Ceram. Soc*. **38**, 3578 (2018).
[61]M. Balcerzak, K. Kawamura, R. Bobrowski, P. Rutkowski and T. Brylewski, Mechanochemical synthesis of (Co,Cu,Mg,Ni,Zn)O high-entropy oxide and its physicochemical properties, *J. Korean Inst. Electr. Electron. Mater. Eng*. **48**, 7105 (2019).
[62]B. Wang, J. C. Yao, J. H. Wang and A. M. Chang, Enhanced structural and aging stability in cation-disordered spinel-type entropy-stabilized oxides for thermistors, *ACS Appl. Electron. Mater*. **4**, 1089 (2022).
[63]Z. W. Zheng, H. M. Ji, Y. W. Zhang, J. H. Cai and C. S. Mo, High-entropy $(Ca_{0.5}Ce_{0.5})(Nb_{0.25}Ta_{0.25}Mo_{0.25}W_{0.25})O_4$ scheelite ceramics with high-temperature negative temperature coefficient (NTC) property for thermistor materials, *Solid. State. Ion*. **377**, 115782 (2022).
[64]K. Edalati, M. Arimura, Y. Ikoma, T. Daio, M. Miyata, D. J. Smith and Z. Horita, Plastic deformation of $BaTiO_3$ ceramics by high-pressure torsion and changes in phase transformations optical and dielectric properties, *Mater. Res. Lett*. **3**, 216 (2015).
[65]D. Bérardan, S. Franger, D. Dragoe, A. K. Meena and N. Dragoe, Colossal dielectric constant in high entropy oxides, *Phys. Status Solidi RRL* **10**, 328 (2016).
[66]S. Zhou, Y. Pu, Q. Zhang, R. Shi, X. Guo, W. Wang, J. Ji, T. Wei and T. Ouyang, *Ceram. Int*. **46**, 7430 (2020).
[67]A. Sarkar, L. Velasco, D. Wang, Q. Wang, G. Talasila, L. de Biasi, C. Kübel, T. Brezesinski, S. S. Bhattacharya, H. Hahn and B. Breitung, High entropy oxides for reversible energy storage, *Nat. Commun*. **9**, 3400 (2018).
[68]Y. Zou, H. Ma and R. Spolenak, Ultrastrong ductile and stable high-entropy alloys at small scales, *Nat. Commun*. **6**, 7748 (2015).
[69]Y. P. Pu, Q. W. Zhang, R. Li, M. Chen, X. Y. Du and S. Y. Zhou, Dielectric properties and electrocaloric effect of high-entropy $(Na_{0.2}Bi_{0.2}Ba_{0.2}Sr_{0.2}Ca_{0.2})TiO_3$ ceramic, *Appl. Phys. Lett*. **115**, 223901 (2019).

[70]Q. Du, J. H. Yan, X. Y. Zhang, J. S. Li, X. Y. Liu, J. R. Zhang and X. W. Qi, Phase evolution and dielectric properties of $Ba(Ti_{1/6}Sn_{1/6}Zr_{1/6}Hf_{1/6}Nb_{1/6}Ga_{1/6})O_3$ high-entropy perovskite ceramics, *J. Mater. Sci: Mater. Electron*. **31**, 7760 (2020).

[71]A. Radon, Ł. Hawełek, D. Łukowiec, J. Kubacki and P. Włodarczyk, Dielectric and electromagnetic interference shielding properties of high entropy (Zn,Fe,Ni,Mg,Cd)Fe_2O_4 ferrite, *Sci. Rep*. **9**, 20078 (2019).

[72]D. A. Vinnik, E. A. Trofimov, V. E. Zhivulin, S. A. Gudkova, O. V. Zaitseva, D. A. Zherebtsov, A. Y. Starikov, D. P. Sherstyuk, A. A. Amirov, A. V. Kalgin, S. V. Trukhanov and F. V. Podgornov, High entropy oxide phases with perovskite structure, *Nanomaterials* **10**, 268 (2020).

[73]D. Lin and K. W. Kwok, Structure, ferroelectric and piezoelectric properties of $(Bi_{1-x-y}Na_{0.925-x-y}Li_{0.075})_{0.5}Ba_xSr_yTiO_3$ lead-free piezoelectric ceramics, *Curr. Appl. Phys*. **9**, 1369 (2009).

[74]R. Zachariasz and D. Bochenek, Modified PZT ceramics as a material that can be used in micromechatronics, *Eur. Phys. J. B* **88**, 296 (2015).

[75]D. Bochenek, P. Niemiec, R. Skulski and M. Adamczyk-Habrajska, Electrophysical properties of a multicomponent PZT-type ceramics for actuator applications, *J. Phys. Chem. Solids* **133**, 128 (2019).

[76]X. Li, J. X. Ma, K. P. Chen, C. W. Li, X. W. Zhang and L. N. An, Design and investigate the electrical properties of $Pb(Mg_{0.2}Zn_{0.2}Nb_{0.2}Ta_{0.2}W_{0.2})O_3$–$PbTiO_3$ high-entropy ferroelectric ceramics, *Ceram. Int*. **48**, 12848 (2022).